ChemComm

Accepted Manuscript

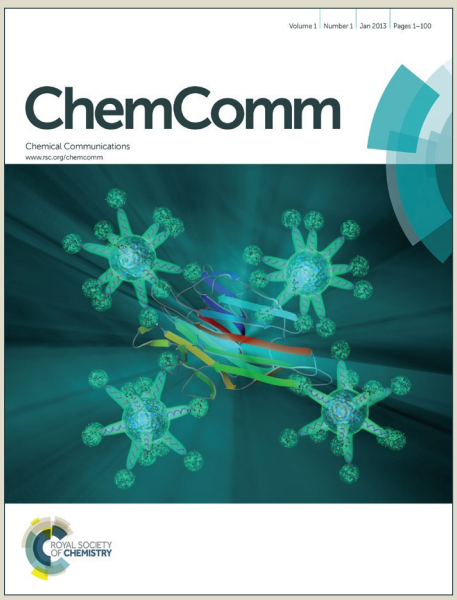

ROYAL SOCIETY OF CHEMISTRY

www.rsc.org/chemcomm

Chemical Communications

COMMUNICATION

Identifying Low-Coverage Surface Species on Noble Metal Nanoparticles by DNP-NMR

Received 00th January 20xx,
Accepted 00th January 20xx

DOI: 10.1039/x0xx00000x

www.rsc.org/

Robert L. Johnson,[a] Frédéric A. Perras,[b] Takeshi Kobayashi,[b] Thomas J. Schwartz,[c] James A. Dumesic,[c] Brent H. Shanks,[a] and Marek Pruski*[b,d]

DNP NMR spectroscopy has been applied to enhance the signal for organic molecules adsorbed on γ-Al_2O_3-supported Pd nanoparticles. By offering >2500-fold time savings, the technique enabled the observation of ^{13}C-^{13}C cross-peaks for low coverage species, which were assigned to products from oxidative degradation of methionine adsorbed on the nanoparticle surface.

Noble metal nanoparticles compose an exciting class of materials with diverse applications including chemical sensing, optical, photothermal, surface-enhanced Raman spectroscopy, and therapeutic applications.[1] One of the most promising uses of these nanomaterials is as heterogeneous catalysts when supported on inert carriers.[2] However, characterization of metal nanoparticles and the reactions occurring on their disordered surfaces with substrate molecules is extremely challenging by conventional means.

Solid-state nuclear magnetic resonance (SSNMR) spectroscopy is uniquely suited for the characterization of many classes of complex amorphous solids, including heterogeneous catalysts with sufficiently high surface area. In such systems, it can yield definite, atomic-level structural information, provide a direct view of the interactions between the adsorbed molecules and active sites, and identify the mechanisms of catalytic transformations.[3]

The low amount of the probe molecules that can be accommodated onto a highly dispersed supported catalyst however poses a major sensitivity challenge for SSNMR, often prohibiting the acquisition of standard one-dimensional (1D) NMR spectra. In cases when the sensitivity can be enhanced by isotopic enrichment, the spectral crowding may limit the utility of 1D spectra. Additional resolution is best achieved by spreading the resonances along a second dimension in two-dimensional (2D) correlation experiments, but such strategy further exacerbates the sensitivity woes.

Recently, important progress has been made in the field of dynamic nuclear polarization (DNP) SSNMR.[4] DNP enables polarization of nuclear spins by the electrons, with which species adsorbed on a surface can obtain signal enhancements of several hundred, or time savings of 3 to 4 orders of magnitude.[5] Although DNP surface-enhanced NMR spectroscopy (DNP-SENS) has previously been applied to studying oxide nanoparticles,[6] the efficacy of this technique for pure metal nanoparticles is still largely unexplored. Potential problems may arise, for example, from the heating of the sample due to spinning of metallic species in a magnetic field or from poor microwave penetration; both effects would lead to a decrease in DNP efficiency. ^{119}Sn DNP SENS experiments have, nonetheless, been recently performed on Sn/SnO_x nanoparticles,[7] but no such experiments have, to the best of our knowledge, been performed on noble metal nanoparticles.

Metal-catalyzed hydrogenation of biologically-derived platform intermediates is a key technology for producing biorenewable chemicals from biomass.[8] Unfortunately, sulfur containing biogenic impurities, such as methionine (Met, an amino acid), are present in the fermentation media, and they can lead to rapid deactivation of reduced metal catalysts.[9] Previous SSNMR studies have been conducted to characterize the poisoned catalyst post-mortem;[10] however, the initial binding and breakdown of Met on the nanoparticle surface could not be elucidated. ^{13}C NMR spectroscopy of post-mortem catalysts showed that methionine had been fragmented, at the sulfur site, producing a variety of carboxylic acids. The strong poisoning effect was attributed to the methylsulfide group remaining bound to the Pd surface, evident from an unusually large ^{13}C chemical shift, when compared to Met on γ-Al_2O_3 without Pd.

The Pd/Al_2O_3 catalysts used in this study were prepared by incipient wetness impregnation of γ-Al_2O_3 (Strem, low-soda) with $Pd(NO_3)_2$ (prepared from Aldrich's 10% $Pd(NO_3)_2$ solution in 10% HNO_3, 99.999%). The catalysts were subsequently dried at 383 K for 2 hours, calcined in flowing air at 673 K (Medical Grade, USP), reduced in flowing hydrogen (Industrial Grade), and passivated with 1% O_2 in Ar (Research Grade). Met-impregnated materials were prepared using uniformly ^{13}C-enriched methionine (Cambridge Isotope Laboratories: L-methionine U-13C5, 97-99%), which was added to samples by incipient wetness impregnation of the reduced

[a] Department of Chemical and Biological Engineering, Iowa State University, Ames, IA 50011-2230, USA
[b] US DOE, Ames Laboratory, Ames, IA 50011-3020, USA
[c] Department of Chemical and Biological Engineering, University of Wisconsin, Madison, WI 53706, USA
[d] Department of Chemistry, Iowa State University, Ames, IA 50011-3020, USA

and passivated Pd/γ-Al_2O_3 catalysts using solutions in D_2O (Aldrich, 99.0 atom% D) and added to catalyst in a 1:1 met:Pd ratio (determined via CO chemisorption). Samples were subsequently dried under vacuum at 318 K for 2 hours.

To understand the early stages of Met binding and breakdown, the Pd/Al_2O_3 catalysts, impregnated with uniformly ^{13}C-enriched Met, were studied using 1D ^{13}C multi-cross-polarization magic angle spinning (multi-CPMAS)[11] NMR spectroscopy, as described caption to Fig. 1. Note that the spectrum of neat Met (Fig. 1a) comprises all expected ^{13}C resonances with quantitative intensities. The same resonances with similar intensities were observed in Met impregnated on the γ-Al_2O_3 support, demonstrating that Met's structure remains intact. This is not the case, however, in the material containing supported Pd nanoparticles (Fig. 1c). The spectrum still features resonances characteristic of intact Met bound to the Pd surface, albeit with a decrease in peak intensity from the α- and methylene carbons, peak broadening, and a high-frequency shift. Interestingly, these spectral changes are accompanied by the emergence of new peaks at 163, 98 and 120-150 ppm, which are not characteristic of either the carboxyl or sp^3-hybridized carbons found in Met, but likely correspond to low-coverage surface species present during the Pd-catalyzed oxidation of Met when exposed to air. The low intensity of the cross-peaks originating from these species prevented us from definitively assigning these shifts based on conventionally acquired 2D NMR spectra (see Fig. 3a).

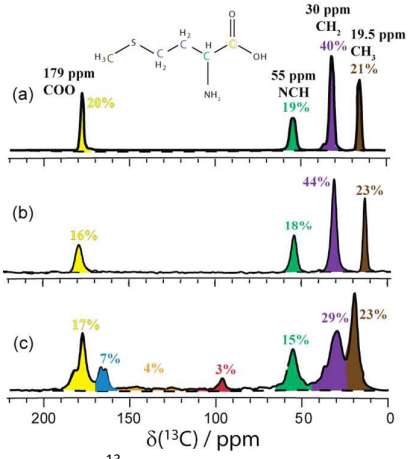

Fig. 1 Conventional 1D ^{13}C multi-CPMAS NMR spectra of Met (a), as well as Met impregnated onto γ-Al_2O_3 (b) and γ-Al_2O_3-supported Pd nanoparticle catalyst (c). The spectra were acquired on a Bruker DSX400 spectrometer equipped with a 4-mm MAS probe. Quantitative ^{13}C NMR spectra were obtained by applying the multi-CPMAS pulse sequence as described previously,[11] using MAS rate of 14 kHz, 4 repolarization cycles with a 0.9 s delay for ^{1}H relaxation, 1.1 ms CP contact times, 2 s recycle delay, and 1536 scans for each spectrum.

To improve our understanding of Met adsorbed on the Pd surface, we have explored the use of DNP-enhanced ^{13}C CPMAS NMR spectroscopy, with biradical polarization agents dissolved in both aqueous (H_2O and AMUPol)[12] and organic (tetrachloroethane (TCE) and TEKPol)[13] solvents. The DNP-enhanced NMR experiments were performed using a Bruker AVANCE III 400 MAS-DNP-NMR spectrometer equipped with a 3.2-mm MAS probe operated at 105 K. Prior to performing the experiments, the samples were impregnated with 16 mM solutions of biradicals and spun at room temperature to evenly distribute the sample within the rotor. As can be seen in Fig. 2, the TEKPol/TCE solution provides a 53-fold signal enhancement, whereas AMUPol provides a signal enhancement by a factor of only 16. A potential disadvantage of TEKPol/TCE is that it produces a strong, albeit non-obstructive, solvent-derived ^{13}C resonance at 75 ppm in the 1D spectra; however, it does not contribute to the 2D ^{13}C-^{13}C correlation signals.

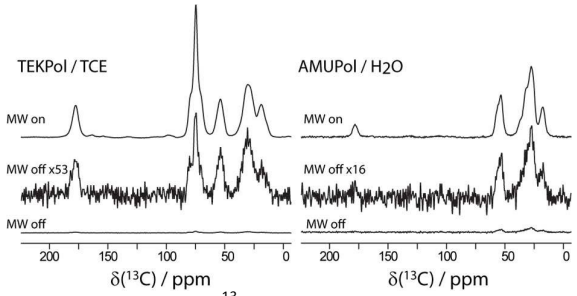

Fig. 2 Comparison of the ^{13}C CP DNP-enhancements of the Met-impregnated, γ-Al_2O_3-supported, Pd nanoparticles obtained using the TEKPol/TCE and AMUPol/H_2O solutions. The measurements were carried out with microwave source 'on' and 'off' as indicated in the figures, under MAS at 12 kHz, using a 2 ms CP contact time, 15 s recycle delay, with 8 scans for TEKPol/TCE and 32 scans for AMUPol/H_2O.

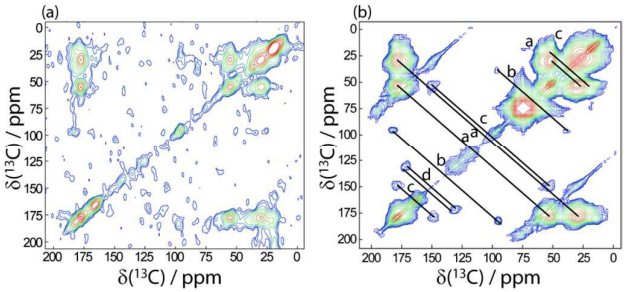

Fig. 3 SQ-SQ DARR ^{13}C-^{13}C correlation spectra of the Met-impregnated, γ-Al_2O_3-supported, Pd nanoparticles acquired using a conventional NMR spectrometer at room temperature (a) and DNP-enhanced measurement at 105 K (b). Both spectra were acquired using a DARR mixing period of 100 ms, under the CP conditions corresponding to 1D spectra in Figs 1 and 2, respectively. The conventional spectrum was acquired in ~14 h (using 132 t_1 increments of 40 μs, 192 scans per increment, and a 2s recycle delay), whereas the acquisition of DNP-enhanced spectrum took 6 h (using 114 t_1 increments of 41.67 μs, 64 scans per increment, and a 3 s recycle delay).

The 2D ^{13}C-^{13}C spin diffusion experiments utilizing dipolar-assisted rotational resonance (DARR) are shown in Fig. 3. The enhancement offered by DNP allows us to clearly observe several minor cross-peaks that are indistinguishable from the noise in the spectrum obtained using a conventional SQ-SQ NMR experiment (Fig 3a). Along with the cross-peaks characteristic of Met, cross-peaks are also observed at unusual chemical shifts, which are listed in Table 1. To better assign these peaks, we additionally performed

a DNP-enhanced refocused-incredible natural-abundance double-quantum transfer experiment (refocused-INADEQUATE)[14] on this sample. In contrast to SQ-SQ measurement discussed above, which yields through-space ^{13}C-^{13}C correlations, the INADEQUATE experiment relies on homonuclear ^{13}C-^{13}C *J* coupling thereby providing a through-bond connectivity map of directly bound nuclei. Additionally, the evolution during t_1 involves only double-quantum (DQ) coherences, which serves to produce simple spectral patterns, free from strong diagonal resonances from non-interacting spins that can hinder the assignment of SQ-SQ spectra. Indeed, the INADEQUATE spectrum revealed a number of cross-peaks near the diagonal that were not observed in the SQ-SQ experiment (see Fig. 4). Namely, we see additional cross-peaks for several different types of methylene groups, and a 168-163 cross-peak.

Table 1. Cross-peaks observed in the DNP-enhanced ^{13}C-^{13}C correlation experiments

$\delta(^{13}C)_a$ / ppm	$\delta(^{13}C)_b$ / ppm	Experiment	Assignment[a]
183	95	both	b
179	149	DARR	c
179	30	DARR	a (long range)[b]
178	52	both	a
173	132	both	d
170	130	both	d
168	163	INADEQUATE	e
151	52	DARR	c
96	39	both	b
53	34	both	a
52	25	both	c
36	29	INADEQUATE	b
33	26	INADEQUATE	a
28	24	INADEQUATE	a

[a] See text and Fig. 5 for the description of the assignments.
[b] Due to the very high intensity of this peak in the DARR spectrum, its absence in the INADEQUATE spectrum suggests that this is a long range correlation.

By comparing the DARR and INADEQUATE spectra, we can develop a more complete picture of the binding of Met to Pd and of the initial oxidative breakdown of Met. Considering the unusual chemical shifts and bonding partners observed, we postulate the existence of several low-coverage species adsorbed on the catalyst surface. Fig. 5 (a-e) shows that these species correspond to Met bound onto the Pd particle surface and species which have been oxidized to various extents. In particular, the cross-peaks from 95 ppm to both 183 ppm and 39 ppm suggest that the partial oxidation of Met may occur at the α-carbon, forming a hemiaminal (Fig. 5b). If, however, oxidation were to occur at the β-carbon, an alcohol adjacent to an imine could be produced (Fig. 5c), which could be the origin of the cross-peaks from ~150 ppm to ~180 ppm and 52 ppm. Oxidative cleavage of the imine to release Pd-bound $S(Me)_2$ would explain the cross-peaks between ~170 ppm and ~130 ppm. Lastly, further oxidation is responsible for the INADEQUATE cross-peaks between 163 and 168 ppm, which we assign to the formation of Pd-bound oxalate, and the 5 ppm change in chemical shift for one of the resonances is in agreement with binding to the Pd nanoparticle surface. Based on these assignments, we postulate that these low-coverage species are intermediates in the oxidative degradation of Met on the Pd surface at ambient conditions. Importantly, the shifts that arising from these species can be weakly observed in the conventional 1D multi-CPMAS spectra; however, there is not sufficient resolution to adequately assign the shifts, and they could not be observed at all in the conventional 2D experiments. Only by the application of 2D DNP-SENS were we able to successfully assign these shifts, demonstrating that this technique is more broadly applicable for the identification of low-coverage species bound to metal nanoparticle surfaces. Whereas the observed shifts and correlations suggest that the methylsulfide and oxalate species (a and e) are Pd-bound, the exact location of other minor species cannot be assessed with certainty.

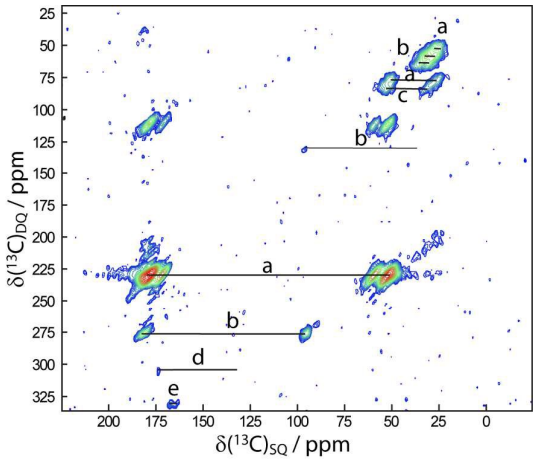

Fig. 4 ^{13}C refocused-INADEQUATE spectrum of the Met-impregnated, γ-Al_2O_3-supported, Pd nanoparticles acquired using DNP-enhancement at 105 K. The cross-peaks are labelled according to Table 1. The experiment used delays lasting 36 rotor periods for double-quantum excitation as well as reconversion, and 110 t_1 increments of 27.78 μs were acquired, each consisting of 256 scans. Other experimental conditions were the same as in the SQ-SQ DARR measurement shown in Fig. 3b.

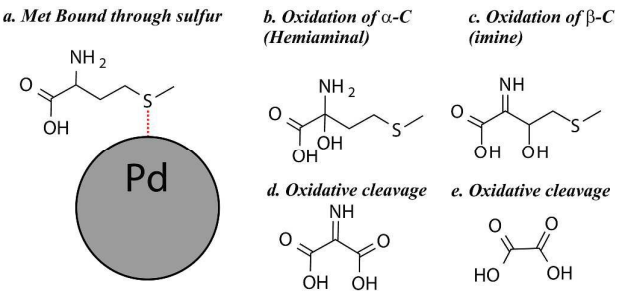

Fig. 5 A scheme showing the stepwise breakdown of Met on the surface of Pd nanoparticles, elucidated using DNP-enhanced ^{13}C-^{13}C correlation NMR.

Conclusions

In conclusion, we have demonstrated the utility of DNP-MAS NMR for studying molecules with low surface coverages reacting on

the surface of supported noble metal nanoparticles in catalyst systems. These experiments can be used to monitor the formation of minor intermediates during catalytic breakdown of a given species, thereby enabling the identification of key sites on the Met molecule which undergo attack from the γ-Al_2O_3-supported Pd nanoparticles. Namely, we observe a sequential oxidation of Met to oxalate and, finaly, carbonate, following a release of Pd-bound methylsulfide. These developments should inspire further work utilising DNP-MAS NMR in understanding the chemistry at the surface of noble metal nanoparticles.

Acknowledgment

The authors are indebted to Dr. K. Schmidt-Rohr for helpful discussuions. This research is supported by the U.S. Department of Energy (DOE), Office of Science, Basic Energy Sciences, Division of Chemical Sciences, Geosciences, and Biosciences and the National Science Foundation Engineering Research Center program (EEC-0813570). Support for F.P. is through a Spedding Fellowship funded by the LDRD program. Ames Laboratory is operated for the DOE by Iowa State University under Contract No. DE-AC02-07CH11358.

Notes and references

1 P. K. Jain, X. Huang, I. H. El-Sayed, and M. A. El-Sayed, *Acc. Chem. Res.* 2008, **41**, 1578; S. Nie, and S.R. Emory, *Science* 1997, **275**, 1102; J. Liu, and Y. Lu, *J. Am. Chem. Soc.* 2003, **125**, 6642.

2 R. Schlögl, and S. B. Abd Hamid *Angew. Chem. Int. Ed.* 2004, **43**, 1628; Y. Jiang, and Q. Gao, *J. Am. Chem. Soc.* 2006, **128**, 716; J, Lu, B. Liu, J. P. Greeley, Z. Feng, J. A. Libera, Y. Lei, M. J. Bedzyk, P. C. Stair, J. W. Elam, *Chem. Mater.* 2012, **24**, 2047. W. Long, N. A. Brunelli, S. A. Didas. E. W. Ping, and C. W. Jones, *ACS Catal.* 2013, **3**, 1700; G. Vilé, N. Almora-Barrios, S. Mitchell, N. López, and J. Pérez-Ramírez, *Chem. Eur. J.* 2014, **20**, 5926.

3 L. E. Marbella, and J. E. Millstone, *Chem. Mater.*, 2015, **27**, 2721.

4 T. Maly, G. T. Debelouchina, V. S. Bajaj, K.-N. Hu, C.-G. Joo, M. L. Mak-Jurkauskas, J. R. Sifigiri, P. C. A. van der Wel, J. Herzfeld, R. J. Temkin, and R. G. Griffin, *J. Chem. Phys.* 2008, **128**, 052211.

5 R. G. Griffin, *Nature*, 2010, **468**, 381; A. Lesage, M. Lelli, D. Gajan, M. A. Caporini, V. Vitzthum, P. Miéville, J. Alauzun, A. Roussey, C. Thieuleux, A. Mehdi, G. Bodenhausen, C. Copéret, and L. Emsley, *J. Am. Chem. Soc.* 2010, **132**, 15459; A. J. Rossini, A. Zagdoun, M. Lelli, A. Lesage, C. Copéret, and L. Emsley, *Acc. Chem. Res.* 2013, **46**, 1942.

6 V. Vitzthum, P. Miéville, D. Carnevale, M. A. Caporini, D. Gajan, C. Copéret, M. Lelli, A. Zagdoun, A. J. Rossini, A. Lesage, L. Emsley, and G. Bodenhausen, *Chem. Commun.*, 2012, **48**, 1988; O. Lafon, A. S. L. Thankamony, M. Rosay, F. Aussenac, X. Lu, J. Trébosc, V. Bout-Roumazeilles, H. Vezin, and J.-P. Amoureux, *Chem. Commun.*, 2013. **49**, 2864; T. Kobayashi, O. Lafon, A. S. L. Thankamony, I. I. Slowing, K. Kandel, D. Carnevale, V. Vitzthum, H. Vezin, J.-P. Amoureux, G. Bodenhausen, and M. Pruski, *Phys. Chem. Chem. Phys.* 2013, **15**, 5553; O. Lafon, A. S. L. Thankamony, T. Kobayashi, D. Carnevale, V. Vitzthum, I. I. Slowing, K. Kandel, H. Vezin, J.-P. Amoureux, G. Bodenhausen, and M. Pruski, *J. Phys. Chem. C* 2013, **117**, 1375; Ü. Akbey, B. Altin, A. linden, S. Özçelik, M. Gradzielski, and H. Oschkinat, *Phys. Chem. Chem. Phys.* 2013, **15**, 20706; F. Blanc, L. Sperrin, D. A. Jefferson, S. Pawsey, M. Rosay, and C. P. Grey, *J. Am. Chem. Soc.* 2013, **135**, 2975; F. A. Perras, T. Kobayashi, and M. Pruski, *J. Am. Chem. Soc.* 2015, **137**, 8336.

7 L. Protesescu, A. J. Rossini, D. Kriegner, M. Valla, A. de Kergommeaux, M. Walter, K. V. Kravchyk, M. Nachtegaal, J. Stangl, B. Malaman, P. Reiss, A. Lesage, L. Emsley, C. Copéret, and M. V. Kovalenko, *ACS Nano* 2014, **8**, 2639.

8 T. J. Schwartz, B. J. O'Neill, B. H. Shanks, J. A. Dumesic, *ACS Catal.* 2014, **4**, 2060.

9 Z. Zhang, J. E. Jackson, D. J. Miller, *Bioresour. Technol.* 2008, **99**, 5873.

10 T. J. Schwartz, R. L. Johnson, J. Cardenas, A. Okerlund, N. A. Da Silva, K. Schmidt-Rohr, and J. A. Dumesic, *Angew. Chem. Int. Ed.* 2014, **53**, 12718; R. L. Johnson, T. J. Schwartz, J. A. Dumesic, K. Schmidt-Rohr, *Solid State Nucl. Magn. Reson.*, under review.

11 R. L. Johnson, K. Schmidt-Rohr, J. Magn. Reson. 2014, 239, 44.

12 C. Sauvé, M. Rosay, G. Casano, F. Aussenac, R. T. Weber, O. Ouari, and P. Tordo, *Angew. Chem. Int. Ed.* 2013, **52**, 10858.

13 A. Zagdoun, G. Casano, O. Ouari, M. Schwarzwälder, A. J. Rossini, F. Aussenac, M. Yulikov, G. Jeschke, C. Copéret, A. Lesage, P. Tordo, and L. Emsley, *J. Am. Chem. Soc.* 2013, **135**, 12790.

14 A. Lesage, M. Bardet, and L. Emsley, *J. Am. Chem. Soc.* 1999, **121**, 10987.